Supporting Information

The Metal-Dependence of Oxalate Decarboxylase Activity

Ellen W. Moomaw,[‡,≠] Alexander Angerhofer,[‡] Patricia Moussatche,[‡] Andrew Ozarowski,[§]

Inés García-Rubio,[⊥] and Nigel G. J. Richards[‡,*]

Contribution from the Department of Chemistry, University of Florida, Gainesville, FL 32611-7200, USA, the National High Magnetic Field Laboratory, Florida State University, 1800 E. Paul Dirac Dr., Tallahassee, FL 32310-3706, USA, and the Laboratorium für Physikalische Chemie, ETH Zürich, CH-8043 Zürich-Hönggerberg, Switzerland

[‡] Department of Chemistry, University of Florida

[≠] Present address: Gainesville State College, 3820 Mundy Mill Road, Oakwood, GA 30566

[§] National High Magnetic Field Laboratory, Florida State University

[⊥] Laboratorium für Physikalische Chemie, ETH Zürich

[*] Correspondence to Department of Chemistry, Box 117200, University of Florida, Gainesville, Fl 32611-7200, 352-392-3601 (Office); 352-846-2095 (Fax), richards@qtp.ufl.edu.

Table S1 Primers used in the construction of WT OxDC and metal-binding OxDC mutants.

Enzyme	Type	Primer Sequence
WT OxDC [a]	Forward	5'-GGAGGAAAC**ATCATATG**AAAAAACAAAATG-3'
WT OxDC [b]	Reverse	5'-GCGGCA**GGATCC**TTATTTACTGCATTTC-3'
E101A	Forward	5'-GCTGCATGGGCTTATATGATTTACGG-3'
E101A	Reverse	5'-GCCCATGCAGCTTCTTTATGCCAGTG-3'
E101D	Forward	5'-GCTGACTGGGCTTATATGATTTACGG-3'
E101D	Reverse	5'-GCCCAGTCAGCTTCTTTATGCTGCCAGTG-3'
E101Q	Forward	5'-GCTCAATGGGCTTATATGATTTACGG-3'
E101Q	Reverse	5'-GCCCATTGAGCTTCTTTATGCCAGTG-3'
E280A	Forward	5'-CCCACGCATGGCAATACTACATCTCC-3'
E280A	Reverse	5'-GCCATGCGTGGGTATTCGGGTGCC-3'
E280D	Forward	5'-GCTCATTGGGCTTATATGATTTACGG-3'
E280D	Reverse	5'-GCCCAATGAGCTTCTTTATGCCAGTG-3'
E280Q	Forward	5'-CCCACCAATGGCAATACTACATCTCC-3'
E280Q	Reverse	5'-GCCATTGGTGGGTATTCGGGTGCC-3'

[a] NdeI restriction site engineered (residues shown in bold).
[b] BamHI restriction site engineered (residues shown in bold)

Table S2 Total metal content and specific activity of the OxDC mutants.[a]

Preparation	Mn	Co	Zn	Fe	Cu	Mg	Specific Activity [b]
WT OxDC	1.87	n.d.[c]	0.51	0.07	0.01	0.01	100%
E101A	0.18	< 0.01	0.17	< 0.01	< 0.01	n.d.[d]	< 0.1%
E101D	0.11	< 0.01	0.08	< 0.01	< 0.01	n.d.[d]	1.0%
E101Q	0.09	< 0.01	0.05	0.30	< 0.01	n.d.[d]	1.3%
E280A	0.67	< 0.01	0.12	< 0.01	< 0.01	n.d.[d]	< 0.1%
E280D	0.64	< 0.01	0.07	0.04	< 0.01	n.d.[d]	0.3%
E280Q	0.73	n.d.[c]	0.11	< 0.01	< 0.01	< 0.01	1.1%
E101Q/E280Q	0.07	< 0.01	0.12	0.04	< 0.01	n.d.[d]	< 0.1%

[a] Metal content is expressed as the number of ions/OxDC monomer.
[b] Activity is expressed relative to that of WT OxDC.
[c] n.d. Not determined. Magnesium content was measured instead of cobalt content.
[d] n.d. Not determined. Cobalt content was measured instead of magnesium content

Table S3 Estimates of size for the oligomeric forms of recombinant, wild type OxDC and OxDC mutants obtained using size exclusion chromatography.

	Actual MW (kDa)[a]	Estimated MW (kDa)[b]	Number of OxDC monomers
Carbonic Anhydrase	29	27	-
Albumin	66	93	-
Alcohol Dehydrogenase	150	103	-
Amylase	200	259	-
Apoferritin	443	433	-
Thyroglobulin	669	579	-
WT OxDC	-	596*, 310	14, 7
E101A	-	589*, 208, 80	13, 5, 3
E101D	-	666	15
E101Q	-	500*, 196	12, 5
E280A	-	603*, 272, 222, 105	14, 6, 5, 3
E280D	-	602	14
E280Q	-	617*, 216	14, 5
E101Q/E280Q[c]	-	572*, 189	13, 4

[a] Values shown are those given for the molecular weight standards.
[b] Estimates obtained from size-exclusion chromatography. Asterix indicates the predominant species observed under the elution conditions.
[c] Double mutant in which Glu-101 and Glu-280 are both replaced by glutamine residues.

EPR Simulations

Overview of spectra and simulations

Figures S1-S7 show the results of the best fits obtained for simulations of the EPR spectra. All simulations were performed with the EasySpin toolbox (*1*) in the MATLAB computing environment (The MathWorks, Natick, MA). Simulations of the EPR spectra for the OxDC E280Q mutant used the following spin Hamiltonian for the Mn(II) sites (S = 5/2, I = 5/2):

$$H = \mu_B g \vec{B} \vec{S} + \vec{I} \hat{A} \vec{S} + \vec{S} \hat{D} \vec{S}$$

For the Zeeman and hyperfine terms, we used isotropic g- and A-tensors while allowing for an anisotropic fine structure (or zero field splitting - ZFS) tensor

$$\hat{D} = \begin{pmatrix} -\frac{D}{3} + E & & \\ & -\frac{D}{3} - E & \\ & & 2D \end{pmatrix}$$

Gaussian distributions of the parameters D and E were also introduced in the simulations, defined here as D- and E-strain. Unresolved super-hyperfine or electron-electron interactions were taken into account using a Gaussian linewidth (called H-strain in the EasySpin toolbox). To better fit the non Gaussian lineshape of the lines at high fields, the simulated spectral features were convoluted with an additional Lorentzian linewidth (parameter “lw” in the tables). These eight independent parameters were varied simultaneously to fit the spectra at different microwave frequencies. Although the simulations accounted well for the six main lines of the spectrum that we associated with the N-terminal site Mn in the enzyme, we needed to introduce a second Mn species to simulate some spectral features of lesser intensity (site X, table S4). Due to its very low intensity and considerable overlap with the main Mn(II) site, the parameters and relative contributions of the second site X should be taken only as approximations.

The best simulations for the E280Q OxDC mutant were obtained with the following parameters:

Table S4: E280Q OxDC Mutant

Mn(II) site	g_{iso}	A (MHz)	*D* (MHz)	*D*-strain (% of *D*)	*E* (MHz)	*E*-strain (% of *E*)	H-strain (MHz)	lw (mT)
N-terminal	2.00088	253	825	40	247	40	20	0.5
X	2.00118	246	1200	40	360	40	40	

A similar set of simulations were performed for EPR spectra of the E101A and E101Q OxDC mutants although the very low Mn concentrations in these samples precluded obtaining reliable spectra of the higher spin manifolds. It was difficult to get spectra for these two OxDC mutants at frequencies other than 406.4 GHz. In both cases, simulations were done assuming two components so as to account for the low-field shoulders visible in the high-field spectra. These results, particularly those for the broader shoulders (named as Y and Z in tables S5 and S6) are tentative, however, and may be revised on the basis of future experiments at lower frequencies and higher spin concentrations. The components given here represent an upper limit for the *D* values of any additional Mn(II) component in these samples, as evident from the absence of relevant spectral features below 2000 G in the X-band spectra of the E101A and E101Q OxDC mutants (Figure S8).

The best simulations for the E101A and E101Q OxDC mutants were obtained with the following parameters:

Table S5: E101Q OxDC Mutant

Mn(II) site	g_{iso}	A (MHz)	*D* (MHz)	*D*-strain (% of *D*)	*E* (MHz)	*E*-strain (% of *E*)	H-strain (MHz)	lw (mT)
C-terminal	2.00086	251	−1100	80	220	80	40	0.5
Y	2.00104	256	−2700	20	350	20	40	

Table S6: E101A OxDC Mutant

Mn(II) site	g_{iso}	A (MHz)	*D* (MHz)	*D*-strain (% of *D*)	*E* (MHz)	*E*-strain (% of *E*)	H-strain (MHz)	lw (mT)
C-terminal	2.00087	254	−1100	80	220	80	40	0.5
Z	2.00099	259	−2700	20	270	20	40	

1. Stoll, S., and Schweiger, A. (2006) EasySpin, a comprehensive software package for spectral simulation and analysis in EPR, *J. Magn. Reson. 178*, 42-55.

Figure S1 High-field EPR spectrum of wild-type OxDC enzyme dissolved in 20 mM hexamethylenetetramine buffer containing 0.5 M NaCl, pH 6, at 386.116 GHz and 10 K. The experimental and simulated spectra are displayed in blue and red, respectively. Note that details of this EPR spectrum have been published elsewhere [Angerhofer, A., Moomaw, E. M., Garcia-Rubio, I., Ozarowski, A., Krzystek, J., Weber, R. T., and Richards, N. G. J. (2007) Multifrequency EPR studies on the Mn(II) centers of oxalate decarboxylase, *J. Phys. Chem. B 111*, 5043-5046] and it is therefore included here merely for ease of comparison.

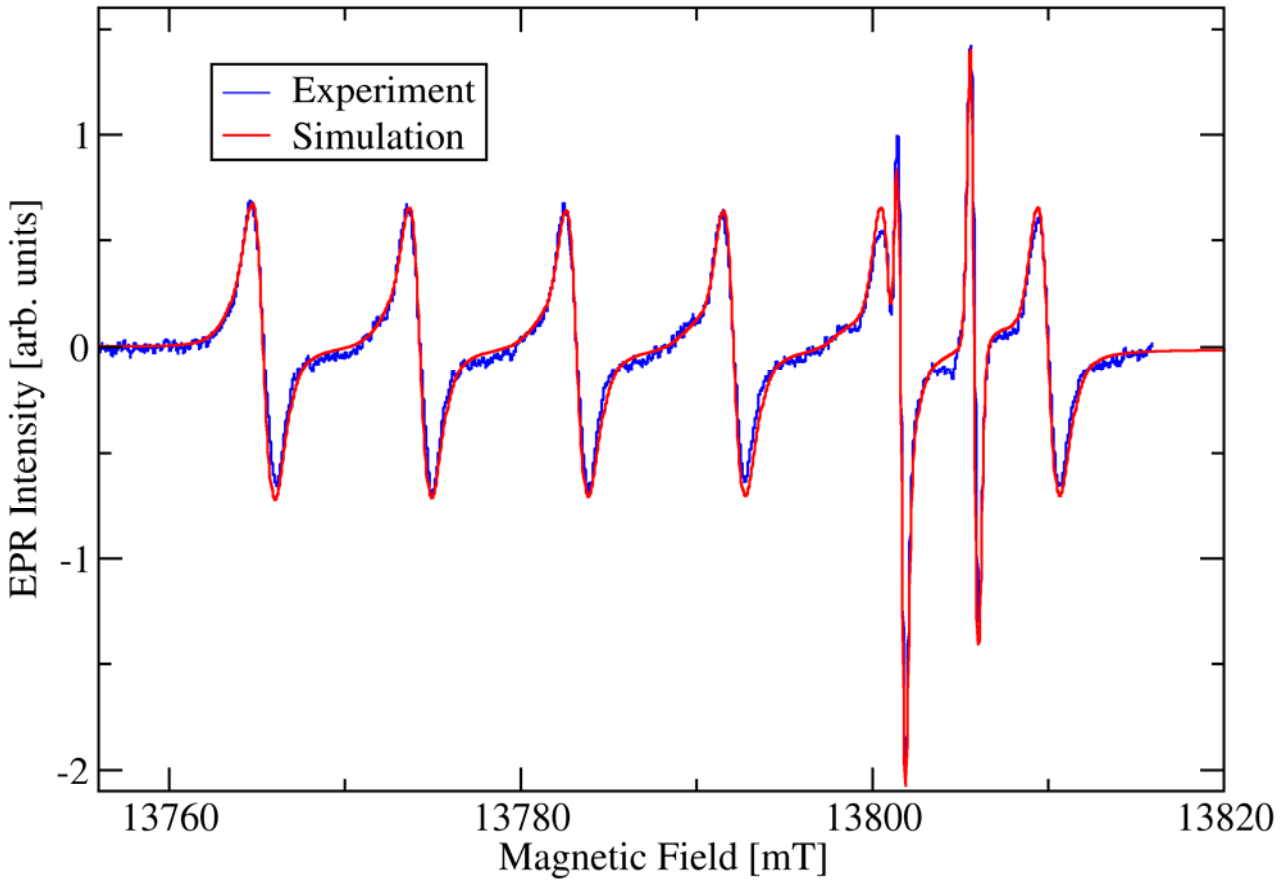

Figure S2 High-field EPR of the E280Q OxDC mutant dissolved in 20 mM hexamethylenetetramine (HMTA) buffer containing 0.5 M NaCl, pH 6, at 382.826 GHz and 50 K at a center field of 13.663 T. The experimental spectrum (microwave power corresponds to 300 mV intensity at the bolometer, modulation frequency 42.5 kHz, modulation amplitude 10.0 G, lock-in sensitivity 500μV, time constant 300 ms, 1 sweep, sweep speed was 0.100 mT/s) is displayed in black, and simulated spectra of the major site (assigned to the N-terminal Mn site) is shown in blue. As explained above, a minority component (green) had to be taken into account in order to account for the low-field shoulders on the main six-line spectrum, contributing approximately 10% of the spectral intensity. The sum of the simulation traces for the two sites is shown in red.

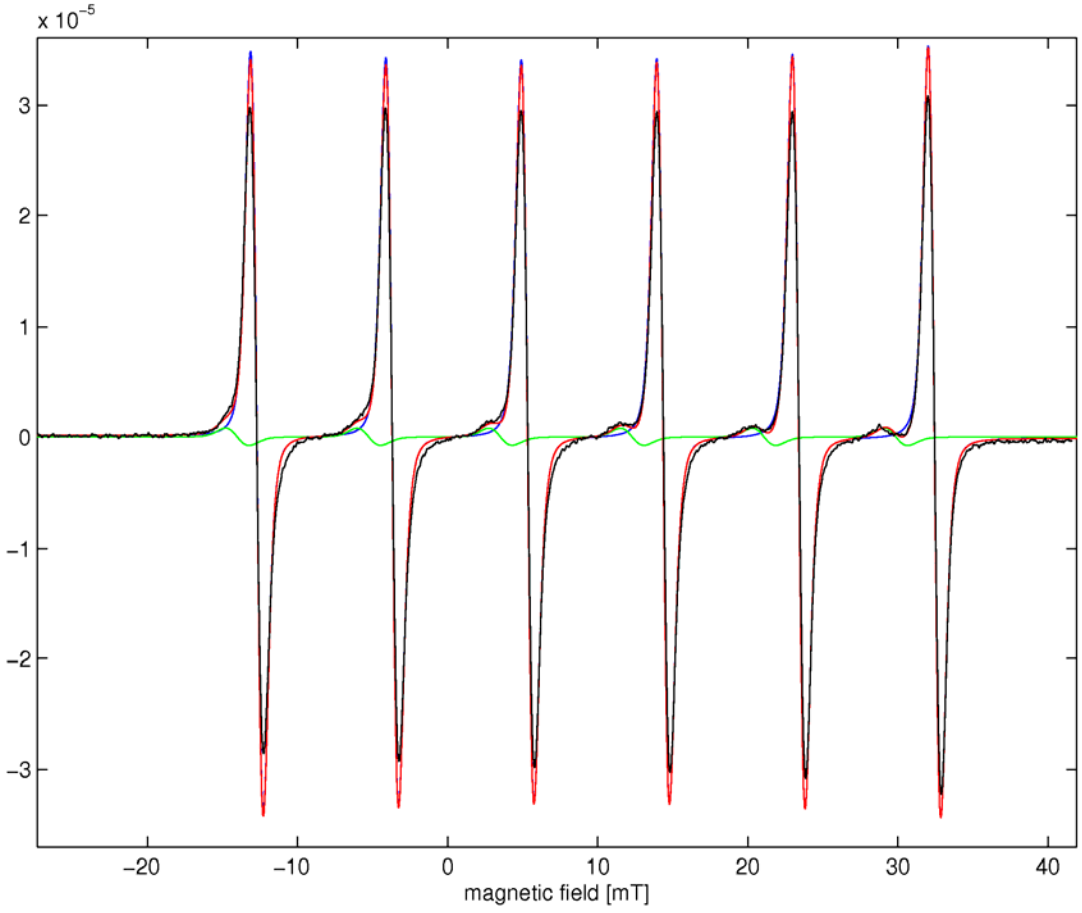

Figure S3 High-field EPR of the E280Q OxDC mutant dissolved in 20 mM HMTA buffer containing 0.5 M NaCl, pH 6, at 331.2 GHz and 20 K. The experimental spectrum (microwave power corresponds to 300 mV intensity at the bolometer, modulation frequency 44.9 kHz, modulation amplitude 16.0 G, lock-in sensitivity 50μV, time constant 100 ms, 1 sweep, sweep speed was 2.00 mT/s) is displayed in black, the simulations of fig. S2 have been scaled to fit the spectrum. Note that dispersion effects close to the strong six-line spectrum may have distorted the experimental trace near 11800 mT to a small degree, explaining the quality of the fit in that region. This spectrum shows that transitions between higher spin manifolds can be observed and that the simulation parameters are consistent with these additional transitions.

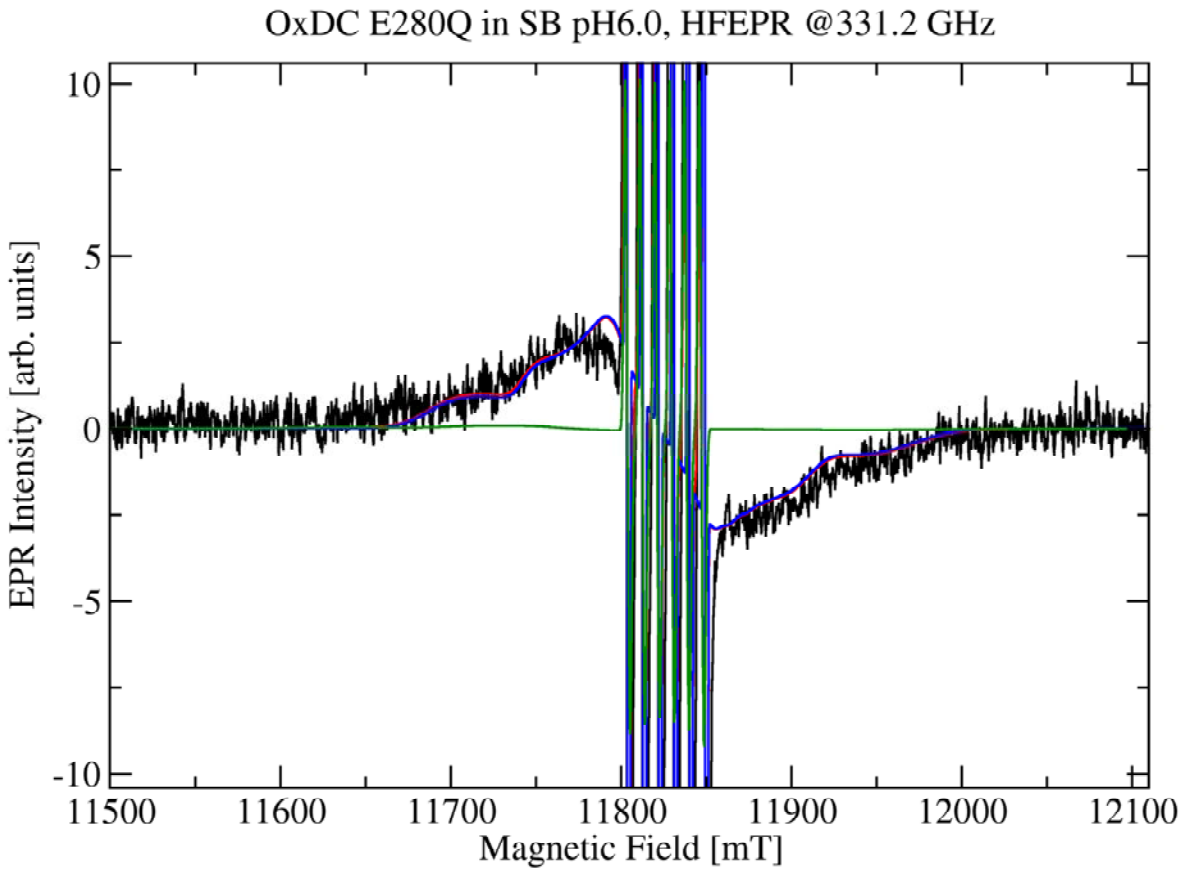

Figure S4 W-band spectrum of the E280Q OxDC mutant dissolved in 20 mM HMTA buffer containing 0.5 M NaCl, pH 6, at 50 K. The experimental spectrum (frequency 94.02002 GHz, microwave power 6.0 µW, modulation frequency 100 kHz, modulation amplitude 2.0 G, receiver gain 40 dB, time constant 82 ms, conversion time 82 ms, 1 sweep, 1.172 G/data point) was taken on a Bruker Elexsys E680 spectrometer, and is displayed in black, and simulated spectra for the N-terminal Mn site (70%) and the additional site (30%) are shown in blue and green, respectively. The sum of the simulation traces for the two sites is shown in red. The contribution of the minor component in green, with its larger fine structure, is very weak and overlaps with the main site, precluding any accurate determination of its magnetic resonance parameters and its relative spin concentration.

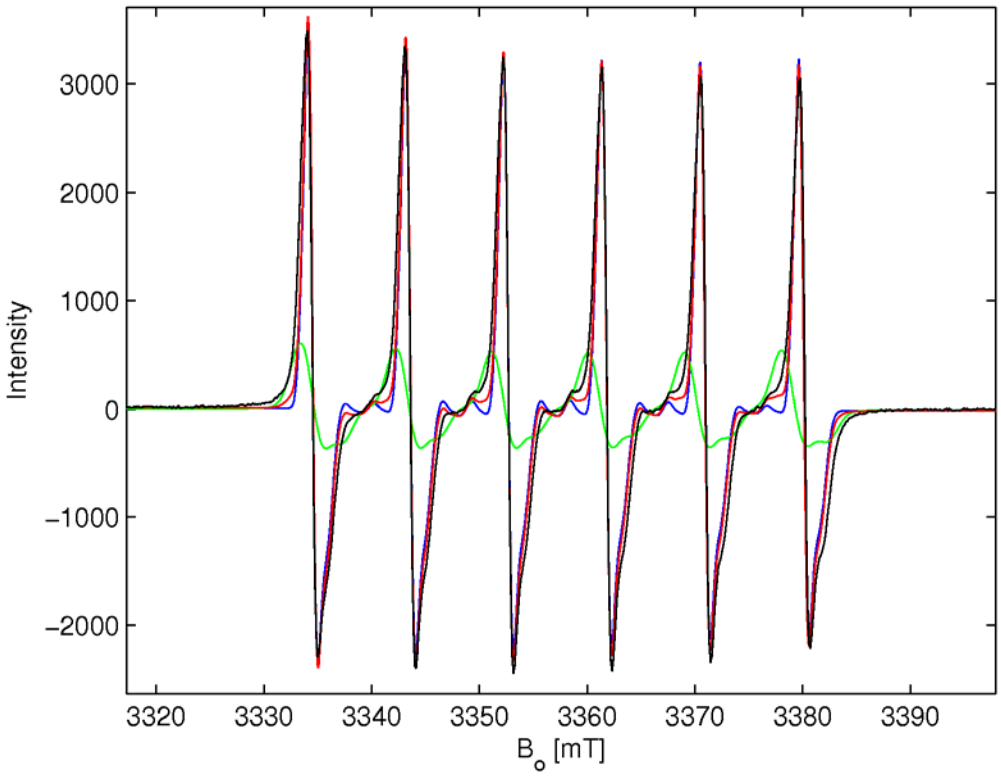

Figure S5 X-band spectrum of the E280Q OxDC mutant dissolved in 20 mM HMTA buffer containing 0.5 M NaCl, pH 6, at 6 K. The experimental spectrum (frequency 9.44521 GHz, microwave power 0.02 mW, modulation frequency 100 kHz, modulation amplitude 10 G, receiver gain 76 dB, time constant 41 ms, conversion time 82 ms, 1 sweep, 0.977 G/data point) was taken on a Bruker Elexsys E580 spectrometer and is displayed in black, and simulated spectra for the N-terminal Mn site (85%) and the second site (15%) are shown in blue and green, respectively. The sum of the simulation traces for the two sites is shown in red.

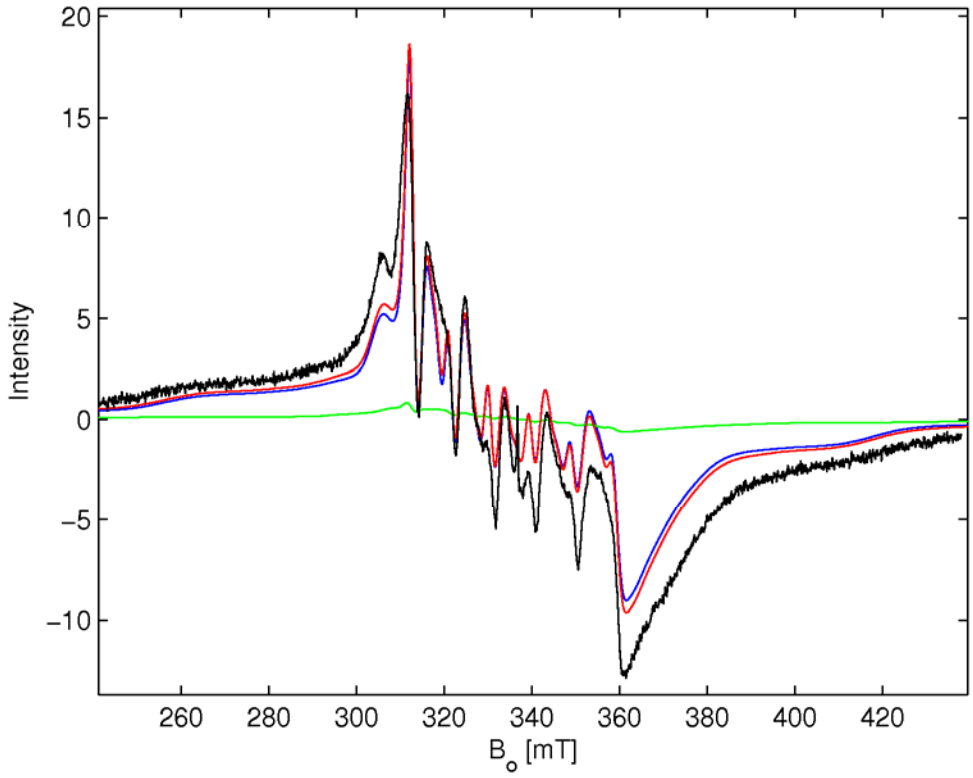

Figure S6: High-field EPR spectra of E101Q OxDC mutant dissolved in 20 mM hexamethylenetetramine (HMTA) buffer containing 0.5 M NaCl, pH 6, at 406.4 GHz and 20 K. The experimental spectrum (microwave power corresponds to 1000 mV intensity at the bolometer, modulation frequency 49.9 kHz, modulation amplitude 1.0 G, lock-in sensitivity 100μV, time constant 3000 ms, 1 sweep, sweep speed was 0.050 mT/s) is displayed in black, and simulated spectra of the two sites are shown in green and blue, respectively. As explained above, the component with large D = −2700 MHz (blue) had to be taken into account in order to account for the low-field shoulders on the main six-line spectrum, contributing approximately 60% of the total spectral intensity. The sum of the simulation traces for the two sites is shown in red. Note: component 2 in the figure corresponds to Y in table S5.

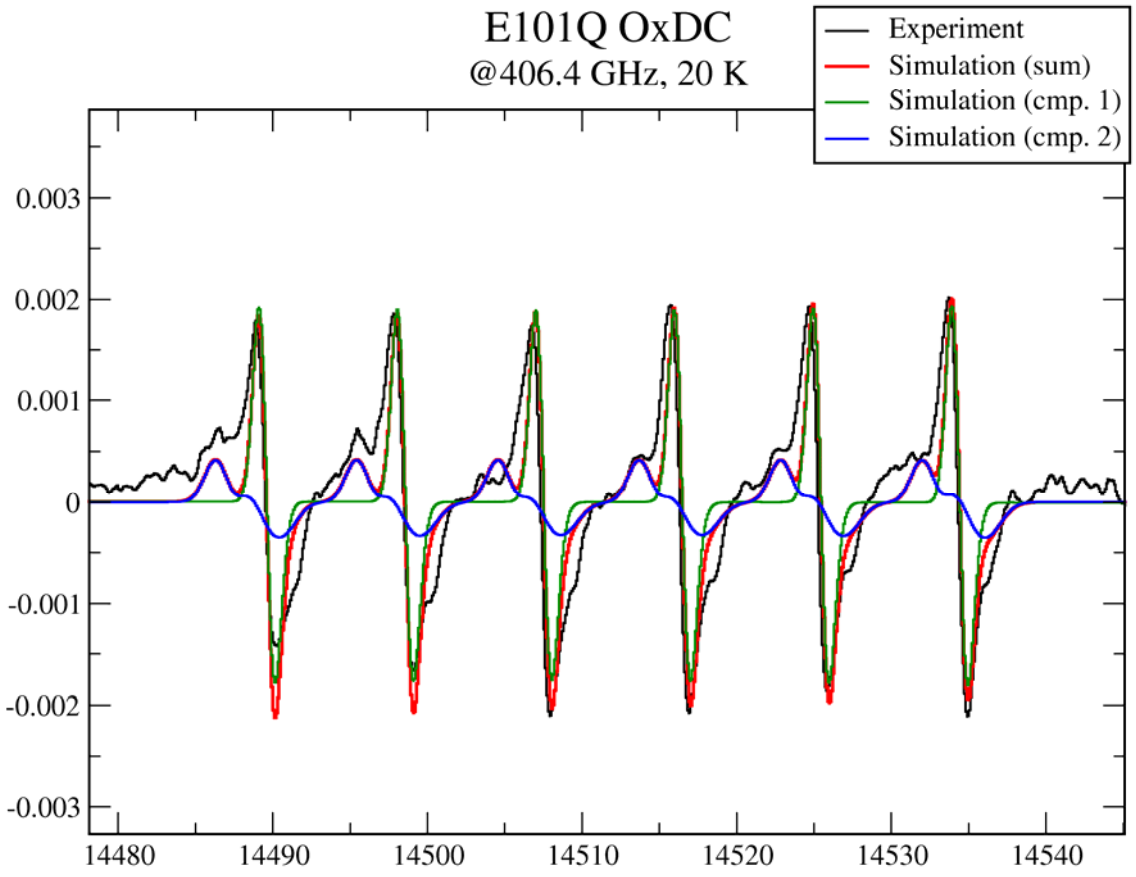

Figure S7: High-field EPR spectra of E101A OxDC mutant dissolved in 20 mM hexamethylenetetramine (HMTA) buffer containing 0.5 M NaCl, pH 6, at 406.4 GHz and 20 K. The experimental spectrum (microwave power corresponds to 1100 mV intensity at the bolometer, modulation frequency 49.9 kHz, modulation amplitude 0.9 G, lock-in sensitivity 200μV, time constant 3000 ms, 1 sweep, sweep speed was 0.40 mT/s) is displayed in black, and simulated spectra of the two sites are shown in green and blue, respectively. As explained above, the component with large D = −2700 MHz (blue) had to be taken into account in order to account for the low-field shoulders on the main six-line spectrum, contributing approximately 30% of the total spectral intensity. The sum of the simulation traces for the two sites is shown in red. Note: Component 2 corresponds to Z in table S6.

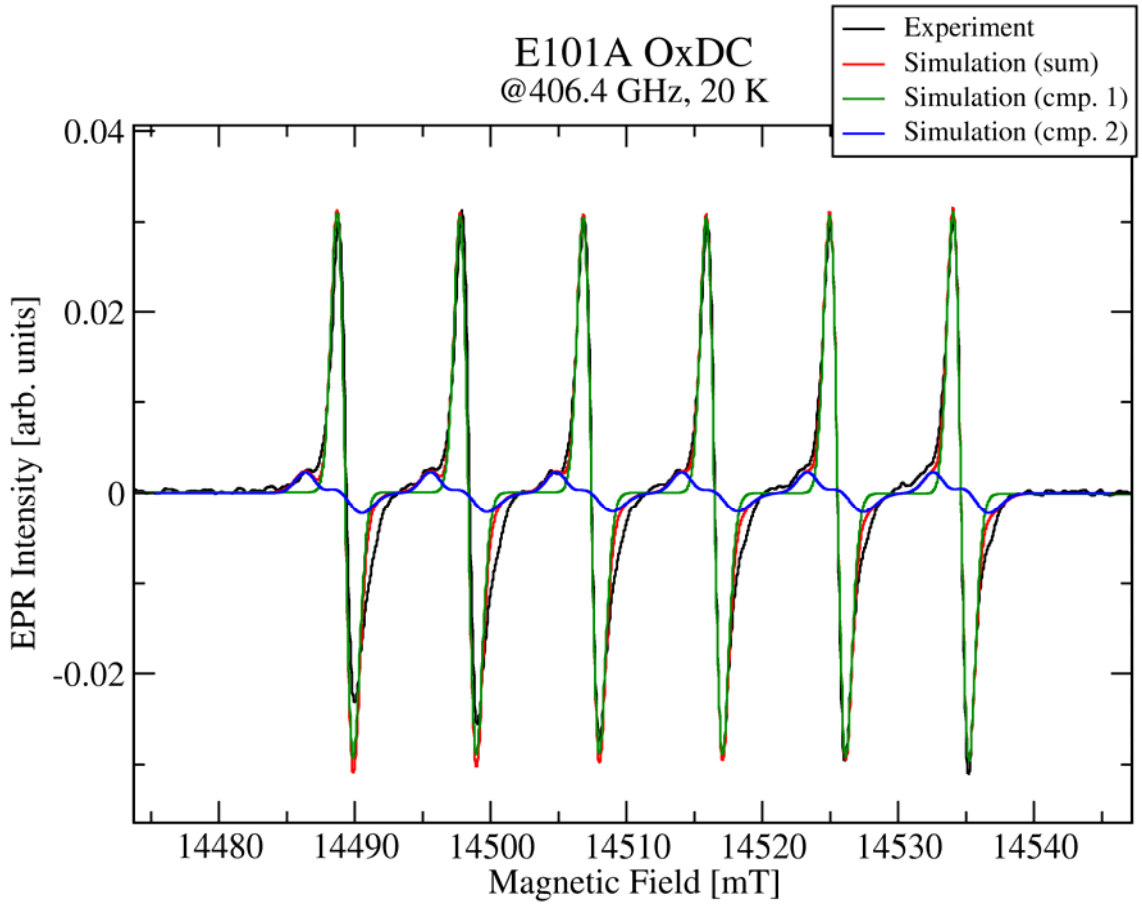

Figure S8: X-band EPR spectra of WT (black), E280Q (red), E101Q (green), and E101A OxDC (blue). All samples were dissolved in 20 mM hexamethylenetetramine (HMTA) buffer containing 0.5 M NaCl, pH 6, and the spectra were taken at 5 K at the following microwave frequencies. WT: ν = 9.439889 GHz; E280Q: ν = 9.440592 GHz; E101Q: ν = 9.442641 GHz, time constant = 1310 ms, conversion time = 2620 ms; E101A: ν = 9.440232 GHz. Unless otherwise noted the following EPR parameters were used: microwave power = 0.2 mW, receiver gain = 65 dB, time constant = 160 ms, conversion time = 320 ms, modulation amplitude = 10 G, 1 scan with 4096 data points. Note the multiplet signal between 1300 and 2000 G in WT which represents a Mn(II) species with very large fine structure (*D* in excess of the microwave quantum) is missing in all the mutants. The weak signal around 1570 G is part of a background signal that could not be completely subtracted. All spectra were baseline corrected by subtracting the spectrum of metal-free buffer solution (the actual flow-through from the concentration step) and normalized to approximately equal peak-to-peak height.

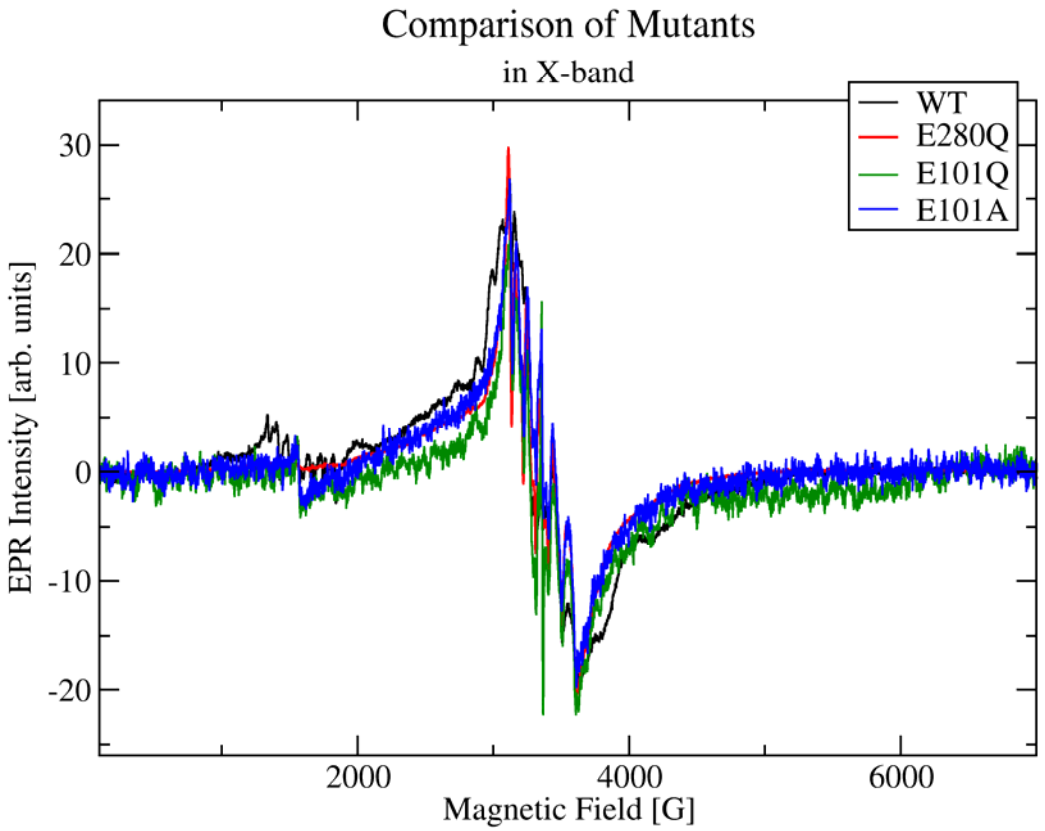

Figure S9 Data for the inversion recovery experiment on wild-type OxDC (12.3 mg/mL), E280Q OxDC mutant (10.8 mg/mL), E101Q OxDC mutant (4.5 mg/mL), and E101A OxDC mutant (3.9 mg/mL). Samples were dissolved in 20 mM HMTA buffer containing 0.5 M NaCl, pH 6.0, and approximately 100 μL total volume of each solution was placed into a quartz tube of 3 mm ID. All spectra were taken at 3700 G (the maximum or the echo-detected EPR spectrum in most samples) and 5 K with microwave frequencies of 9.711321 GHz (WT), 9.7009929 GHz (E280Q), 9.716124 GHz (E101Q), and 9.708295 GHz (E101A). The experiment employed the usual π-T-π/2-τ-π Hahn echo-detected inversion recovery pulse sequence with 16 and 32 ns pulses for π/2 and π pulses, respectively. A 2-phase CYCLOPS sequence was used to separate the echo from artifacts and unwanted spurious echoes. Simulations were performed using a bi-exponential model taking data points after the decay of echo modulations. The results of the simulations are given in the legend as T_1 (% contribution to total intensity).